

# Measuring Global Galaxy Metallicities Using Emission Line Equivalent Widths

Henry A. Kobulnicky

*Department of Physics & Astronomy  
University of Wyoming  
Laramie, WY 82071  
Electronic Mail: chipk@uwyo.edu*

Andrew C. Phillips

*University of California, Santa Cruz  
Lick Observatory/Board of Studies in Astronomy  
Santa Cruz, CA, 95064  
phillips@ucolick.org*

;Final Revised draft of 27 August 2003

Accepted for Publication December 2003 in *The Astrophysical Journal*

## 1. Introduction

Abundances of chemical elements in galaxies are commonly measured using the emission lines emitted by astrophysical nebulae (e.g., see Osterbrock 1989). Recombination lines of hydrogen (e.g., the Balmer series) or helium and forbidden lines of singly and doubly ionized carbon, nitrogen, oxygen, neon, and sulfur are among the strongest observable lines in the visible and ultraviolet spectrum. The relative strengths of each emission line, combined with some knowledge of the temperature and density of the nebulae, provide information about the relative and absolute abundances of each ion. Chemical analyses of individual nebulae have been used to test nucleosynthesis models of stars, the chemical evolutionary history of galaxies, and nucleosynthesis in the big bang (review by Aller 1990; Pagel 1998). Even integrated spectra of entire galaxies may be used to estimate the overall degree of chemical enrichment of a galaxy (Kobulnicky, Kennicutt, & Pizagno 1998).

Observational techniques sometimes permit the relative fluxes of emission lines from galaxies to be measured with a high degree of precision. However, in the current generation of wide-field galaxy surveys on multi-object spectrographs, flux calibration is frequently problematic due to unfavorable observing conditions or instrumental effects such as a variation in system response over the field of view. In addition, the traditional line ratio for reddening determination is  $H\alpha/H\beta$ , but for redshifts greater than  $z \sim 0.3$  the  $H\alpha$  line is not available, and these galaxies rarely have sufficient signal-to-noise in their spectra to attempt a reddening derivation from the higher-order Balmer lines. For such surveys, it is still desirable to extract chemical information from the data, where possible.

In this paper we explore the possibility of estimating mean gas-phase oxygen abundances for galaxies based the *equivalent widths* (rather than fluxes) of strong Balmer  $H\beta$  recombination line and forbidden [O II] and [O III] emission lines. This method essentially uses the underlying stellar continuum as a crude flux calibrator, and has the advantage that any reddening affecting the stars and gas equally will be automatically removed. While we would not expect the equivalent-width method to be as accurate as the traditional method, particularly for individual objects, we find that it works sufficiently well to enable us to measure approximate oxygen abundances in relatively faint, intermediate-redshift galaxies.

Our approach is to develop the method from basic principles, and to test and empirically calibrate it using three spectroscopic galaxy datasets, and in the end compare the oxygen abundance indicator  $R_{23}$  to the quantity  $EW R_{23}$  derived from traditional line fluxes and flux ratios to results using only the equivalent widths and equivalent width ratios. The thesis of this paper is that even when the dereddened line *flux* ratio  $R_{23}$  is not available, a corresponding ratio of *equivalent widths* can still provide an estimate of the oxygen abundance.

This new method is applied to the study of abundances in a set of intermediate-redshift galaxies observed as part of the Deep Extragalactic Evolutionary Probe (DEEP) spectroscopic survey in the Groth Strip (DGSS) presented in a companion paper, Kobulnicky *et al.* (2003; Ke03).

## 2. Gas-phase Oxygen Abundance Measurements from Emission Lines

Standard techniques for measuring chemical abundances in astrophysical nebulae from the fluxes and flux ratios of nebular emission lines are reviewed in Osterbrock (1989). The most direct and reliable techniques involve measuring a suite of temperature-sensitive and density-sensitive line ratios to determine the physical conditions of the plasma. In the absence of high signal-to-noise data measuring temperature-sensitive line ratios (e.g., [O III]  $\lambda 4363$ /[O III]  $\lambda 5007$ ), the default diagnostic for measuring the oxygen abundance of ionized nebulae has become the ratio of strong oxygen emission lines  $R_{23} \equiv (I_{3727} + I_{4959} + I_{5007})/I_{H\beta}$  (Pagel *et al.* 1979). Subsequently, many authors have developed formulations relating this strong line ratio to the gas-phase oxygen abundance (e.g., Edmunds & Pagel 1984; McCall, Rybski & Shields 1985; Dopita & Evans 1986; McGaugh 1991). Most modern calibrations relating  $R_{23}$  to oxygen abundance include a measure of the ionization parameter, such as  $O_{32} \equiv (I_{4959} + I_{5007})/I_{3727} \equiv I_{[O III]}/I_{[O II]}$  as a second parameter (e.g., McGaugh 1991; Pilyugin 2001).

While the  $R_{23}$  method was developed primarily for individual HII regions, Kobulnicky, Kennicutt, & Pizagno (1998; KKP) have shown that this approach is valid even when applied to the integrated spectra of galaxies as a means of estimating an average O/H abundance for the galaxy as a whole. Even when the signal to noise ratio of these lines is as low as 8:1 or when a spectroscopic observation encompasses a range of metallicities and ionization conditions within a galaxy, this ratio provides a rough, but reliable, estimate of the mean gas-phase oxygen abundance when used in

conjunction with the appropriate calibration relating  $R_{23}$  to  $O/H$ . At this signal-to-noise ratio, the associated uncertainty on the oxygen abundance due to line measurement error is typically comparable to the uncertainty due to the calibration of the  $R_{23}$  vs.  $O/H$  relationship:  $\sim 0.15$  dex. In this paper we show that the uncertainty introduced by substituting emission line equivalent widths is less than these other sources of uncertainty, and thereby establish a new method for measuring interstellar medium oxygen abundances.

### 3. Justification of the Equivalent Width Method

The original  $R_{23}$  method involves line ratios, so we consider the effects of using equivalent width ratios in place of flux ratios. For generality, we include the effects of reddening in the discussion, assuming the traditional “screen” model. The equivalent width<sup>1</sup> can be written as

$$W_\lambda = \frac{F_{\lambda 1}}{F_{C\lambda 1}}, \quad (1)$$

where  $F_\lambda$  represents the line flux and  $F_{C\lambda}$  is the underlying continuum flux. The fluxes do not need to be calibrated, since the calibration affects both quantities equally. The dereddened, calibrated flux value for a line,  $I_\lambda$ , or continuum,  $F_\lambda^0$ , is given by

$$I_\lambda = F_\lambda^0 = F_\lambda \times 10^{c(1+f(\lambda))}, \quad (2)$$

where  $c$  is the logarithmic attenuation at  $H\beta$  and  $f(\lambda)$  is a function describing the reddening curve (see Seaton 1979). Combining these leads to a general line ratio formulation of

$$\frac{I_{\lambda 1}}{I_{\lambda 2}} = \frac{W_{\lambda 1} F_{C\lambda 1}}{W_{\lambda 2} F_{C\lambda 2}} 10^{c(f(\lambda 1)-f(\lambda 2))} = \frac{W_{\lambda 1}}{W_{\lambda 2}} \alpha, \quad (3)$$

where we group all the continuum and reddening terms into the factor  $\alpha$ . Note that the continuum will be attenuated by an amount characterized by  $c^*$ , and reddened by (presumably) the same reddening law. Thus,

$$\alpha = \frac{F_{C\lambda 1}^0}{F_{C\lambda 2}^0} 10^{(c-c^*)(f(\lambda 1)-f(\lambda 2))}. \quad (4)$$

The factor  $\alpha$  contains two unknowns, the ratio of the non-reddened continuum fluxes, which depends on the underlying stellar population, and the difference in the attenuation of the emitting gas and the continuum light. Note that values of  $c$  can range from zero to quite large for individual HII regions, although large values are severely deweighted in the average over an entire galaxy. Typical derived values are in the range 0 to 1, with a median value around 0.3 (McCall *et al.* 1985; Olofsson 1995). Values of  $c^*$  can be estimated from the relation  $c^* = 1.47E_{B-V}$  from Seaton. For

---

<sup>1</sup>We adopt the sign convention that emission line equivalent widths are positive.

$E_{B-V}$  in a typical range of 0–0.2,  $c^* \sim 0$ –0.3. In physically realistic situations, we would expect some correlation of  $c$  and  $c^*$ , and also that  $(c - c^*) \geq 0$ .

Let us now consider the specific line ratios of interest for the  $R_{23}$  method. The first is  $I_{[O III]}/I_{H\beta}$ . For the purposes of reddening correction, we adopt the wavelength of the stronger [O III]  $\lambda 5007$  line. The value of  $\alpha$  in this case is

$$\alpha_{\beta 3} = \frac{F_{C5007}^0}{F_{C4861}^0} 10^{(c-c^*)(-0.034)}. \quad (5)$$

Due to the proximity of these emission lines in wavelength, we expect the flux ratios of the underlying stellar population to be very close to unity. Similarly, for realistic  $0 < (c - c^*) < 1$ , the reddening factor will be between unity and 0.92. Thus, for this line ratio,  $\alpha \simeq 1$ , and we will ignore it in further discussion. To a very good approximation,

$$\frac{I_{[O III]}}{I_{H\beta}} \simeq \frac{W_{[O III]}}{W_{H\beta}}. \quad (6)$$

The second ratio,  $I_{[O II]}/I_{H\beta}$ , is more problematic; for these lines,

$$\alpha_{2\beta} = \frac{F_{C3727}^0}{F_{C4861}^0} 10^{(c-c^*)(0.255)}. \quad (7)$$

In principle, we could estimate  $\alpha_{2\beta}$  from a detailed spectral analysis of the flux-calibrated, integrated stellar spectrum and Balmer line ratios, but for faint, galaxies with redshifts  $z > 0.3$  we will have neither the signal-to-noise nor access to the  $H\alpha$  line in order to do this. In practice, we need to adopt an appropriate average value of  $\alpha_{2\beta}$  determined by other means.

Galaxy light tends to be dominated by A main sequence and G and K giants (e.g., Morgan & Mayall 1957; Pritchet 1977; Kobulnicky & Gebhardt 2000), and assuming an underlying stellar spectrum composed of a linear combination of these two spectral types implies that the dereddened flux ratio of the continuum ranges from  $\sim 1$  for late-B stars to  $\sim 0.4$  for mid-G giants to  $\sim 0.2$  for early-K giants (although galaxies whose  $\lambda 3727$  flux is dominated by K stars is unlikely to have any line emission from star formation). Examining the spectra in Kennicutt (1992b) shows the  $\lambda 3727$ -to- $\lambda 4861$  ratio of the continuum fluxes in galaxies with obvious emission lines ranging from  $\sim 0.4$ –1.0; if these were dereddened the range would shift upwards and might possibly narrow somewhat.

On the other hand, the reddening correction ranges from 1 to 1.8 for realistic values  $0 \leq (c - c^*) \leq 1$ , with a typical likely difference  $(c - c^*) \sim 0.3$  giving a reddening factor of  $\sim 1.2$ . Combining the reddening and stellar population factors leads to an expected value of  $\alpha_{2\beta} \sim 0.84 \pm 0.3$ . This expected average value for  $\alpha_{2\beta}$  differs from unity by less than 0.1 dex.

We find the  $R_{23}$  measure can now be expressed

$$R_{23} = \log \frac{I_{[O II]} + I_{[O III]}}{I_{H\beta}} = \log \frac{\alpha_{2\beta} W_{[O II]} + W_{[O III]}}{W_{H\beta}}. \quad (8)$$

Not surprisingly, the  $R_{23}$  measured using equivalent widths and an adopted average value for  $\alpha_{2\beta}$  will be most in error when [O II] dominates [O III].

The final line ratio of interest is the ionization parameter, and it is easy to see that

$$\frac{I_{[\text{O III}]}}{I_{[\text{O II}]}} \simeq \frac{W_{[\text{O III}]}}{\alpha_{23}W_{[\text{O II}]}}. \quad (9)$$

The value  $\alpha_{23} \simeq \alpha_{2\beta}$  to a very good approximation, so at this point we will drop the subscripts and simply refer to “ $\alpha$ ” for either of these quantities. Comparing the ratios above is probably the easiest means to empirically estimate an average value for  $\alpha$ . While it would be equally valid to estimate  $\alpha$  from the [O II] and H $\beta$  ratios, the H $\beta$  equivalent width can be contaminated by underlying stellar absorption.

#### 4. Data Selection and Analysis

In order to empirically measure an average value of  $\alpha$  and to confirm the validity of using equivalent width line ratios in estimating  $R_{23}$ , we compiled three sets of emission-line spectra of nearby galaxies. The first set consists of 16 objects with spatially-integrated spectra from the 55-object spectroscopic galaxy atlas of Kennicutt (1992a,b; K92) plus six additional emission-line objects from KKP. We refer to this sample as the K92+ sample. The K92+ spectra are produced by drifting a longslit across each galaxy and have spectral resolutions of 5-7 Å (K92) and 3 Å (KKP). The 16 K92 galaxies in our subsample are the strongest emission-line objects where global metallicity measurements are possible. The full set of K92 galaxies represents a range of morphological types from Sa to Im, but it includes only the bright galaxies of each type. The KKP galaxies are all underluminous, dwarf emission-line galaxies. For a second local sample, we examined the 198-galaxy Nearby Field Galaxy Survey (Jansen *et al.* 2000a,b; NFGS), which is selected from the CfA redshift catalog (Huchra *et al.* 1983). From this spatially-integrated spectroscopic survey, we culled 98 objects with measurable H $\beta$ , [O III] and [O II] emission lines. These spectra have a resolution of 6 Å and include a larger range of luminosity ( $-14 < M_B < -22$ ) and surface brightnesses than K92+ while spanning morphological types. The K92+ objects have a higher fraction of star-forming galaxies (objects with strong emission lines) compared to the NFGS sample. As a third local sample, we used emission-line selected galaxies in the Kitt Peak National Observatory Spectroscopic Survey (KISS; Salzer *et al.* 2000). KISS is a large-area objective prism survey of local ( $z < 0.09$ ) galaxies selected by strong H $\alpha$  emission, and thus, preferentially contains objects with active star formation. While high-quality slit spectroscopy has been obtained for  $\sim 519$  KISS galaxies (Melbourne & Salzer 2002), 396 galaxies lack [O II] measurements, leaving 123 galaxies. These remaining spectra have 5–8 Å resolution, and are analyzed in Salzer *et al.* (2003).

In summary, the 22 K92+, 98 NFGS, and 123 KISS galaxies were selected from their larger parent samples because of strong emission lines suitable for nebular metallicity measurement. Following KKP, we chose only galaxies with detectable [O II] $\lambda$ 3727, [O III] $\lambda$ 4959, [O III] $\lambda$ 5007, and

$H\beta$  emission lines. Only galaxies where all four emission lines were measured with a S/N of 8:1 or greater were retained. This selection criterion preferentially includes galaxies with high equivalent width lines, but it also includes galaxies with low equivalent width lines where the continuum is smooth and well-measured.

For each galaxy in the K92+ sample we measured the emission-line fluxes and equivalent widths manually using Gaussian fits. For the NFGS and KISS surveys, we adopted the published emission-line fluxes and equivalent widths. Dereddened emission-line fluxes were computed for all three samples by comparing the observed  $F_{H\alpha}/F_{H\beta}$  ratios to theoretical ratios.<sup>2</sup> The line fluxes are dereddened using the law of Seaton (1979) as parameterized by Howarth (1983) and as described in Kobulnicky & Skillman (1996). We did not correct the Balmer emission lines for underlying stellar absorption. The effects of Balmer absorption by the stellar population are discussed in Section 5.3

While the K92+KKP sample consists entirely of starforming galaxies, several low-level AGN are known to exist in the NFGS. These four objects are not included in the our subsample. The 123 KISS galaxies included here do not contain any AGN, as they were selected to be conventional starforming galaxies based on analysis high-quality spectroscopic observations (Salzer 2003). In any case, the presence of AGN among the samples would not have a significant bearing on the results of this paper since we are interested in comparing observable properties of emission lines rather than deriving physical quantities such as density or metallicity which are sensitive to the nature of the ionizing source.

## 5. Analysis of Emission Line Quantities

### 5.1. [O II] and [O III] Equivalent Widths versus Fluxes

Figure 1 compares the oxygen and hydrogen emission-line flux ratios to equivalent width ratios as a function of emission line strength and  $B - V$  color for the K92+ and NFGS samples. Solid symbols denote the Nearby Field Galaxy Sample while crosses denote the K92+ galaxies. The upper left panel compares the ratio of dereddened [O II] to  $H\beta$  fluxes,  $I_{[O II]}/I_{H\beta}$ , versus the ratio of [O II] to  $H\beta$  equivalent widths,  $W_{[O II]}/W_{H\beta}$ . A solid line marks the 1-to-1 correspondence. There is a good correlation between the two quantities, indicating that strong-line equivalent widths are a good surrogate for dereddened line fluxes. The RMS deviation from the 1-to-1 correspondence is  $\sigma(\log[W_{[O II]}/W_{H\beta}]) = 0.11$  dex for the combined K92+NFGS samples. Similarly, the panel at top right shows the  $I_{[O III]}/I_{H\beta}$  versus  $W_{[O III]}/W_{H\beta}$  ratios and indicates that these equivalent width ratios are an excellent substitute for dereddened line fluxes, as expected. The RMS deviation from the 1-to-1 correspondence is  $\sigma(\log[W_{[O III]}/W_{H\beta}]) = 0.05$  dex for the combined K92+NFGS samples.

---

<sup>2</sup> $I_{H\alpha}/I_{H\beta} = 2.75$ - $2.86$  for wide temperature range, e.g., (Hummer & Storey 1987). Here we assumed fixed electron temperature of 12,000 K so that  $I_{H\alpha}/I_{H\beta} = 2.85$ .

The lower panels of Figure 1 show residuals from the 1-to-1 line as functions of  $W_{H\beta}$ ,  $W_{[O\ II]}$ , the ratio  $W_{[O\ III]}/W_{[O\ II]}$  and galaxy color. The K92+ and NFGS galaxies have very small residuals in the right column which compares [O III] to  $H\beta$  ratios. Although small, the NFGS residuals are slightly systematic, with an offset of 0.07 dex. The excellent correspondence of [O III] fluxes to equivalent widths may be easily understood since the [O III]  $\lambda\lambda 4959, 5007$  lines are close in wavelength to  $H\beta$  so that neither changes in the underlying galaxy continuum light nor relative extinction will alter this ratio. The same data is shown for the [O II] to  $H\beta$  ratios in the left column. Here, the K92+ and NFGS galaxies have small, slightly-systematic residuals, particularly as a function of color. In these cases,  $\alpha$  is unlikely to be quite near to unity. There seems to be a systematic offset between the NFGS and K92+ sample, possibly caused by a systematic overestimate of the reddening correction to the [O II]  $\lambda 3727$  flux due to low spectral resolution in the K92 atlas. Within the NFGS sample, the largest residuals are seen in the reddest galaxies, consistent with expectations that the reddest galaxies will have the smallest value of  $\alpha$  (see Equation 9). The systematic trend seen in the residuals with respect to  $W_{H\beta}$  is most likely a reflection of a correlation between  $W_{H\beta}$  and color, i.e., redder galaxies have relatively less star formation and hence relatively weaker  $W_{H\beta}$ . These same galaxies with low  $W_{H\beta}$  will also be the most affected by lack of correction for underlying stellar absorption. Nevertheless, the bulk of the residuals are near zero, indicating that  $\alpha$  has a typical value near unity.

Figure 2 shows the same comparison as Figure 1 but now for the KISS and K92+ samples. There appear to be somewhat more scatter in the KISS sample than in NFGS, and here the RMS deviation from the 1-to-1 correspondence is  $\sigma(\log[W_{[O\ II]}/W_{H\beta}]) = 0.15$  dex and  $\sigma(\log[W_{[O\ III]}/W_{H\beta}]) = 0.04$  dex for the combined K92+KISS samples.

The lower panels of Figure 2 show residuals from the 1-to-1 line as a function of equivalent width and galaxy color. The right column shows very small and non-systematic residuals, indicating excellent correspondence between [O III] equivalent widths and fluxes for all KISS galaxy colors and line ratios. However, the left column shows significant dispersion of 0.15 dex between  $\log[W_{[O\ II]}/W_{H\beta}]$  and  $\log[I_{[O\ II]}/I_{H\beta}]$ . The residuals are not correlated with galaxy color or equivalent width, suggesting that measurement errors and/or uncertainties in the reddening correction are responsible for the dispersion. The [O II]/ $H\beta$  residuals appear slightly offset from the zero line, indicating  $\alpha$  slightly above unity on the average.

## 5.2. The Ionization Parameter [O III]/[O II]

We consider next the ratio of the [O II] and [O III] lines, as this was shown to be the most direct way to estimate the unknown value  $\alpha$ . In addition, the quantity  $I_{[O\ III]}/I_{[O\ II]}$  is a measure of the “hardness” of the ionizing photons, and is used in the  $R_{23}$  to O/H conversion. Modern calibrations relating  $R_{23}$  to oxygen abundance include a measure of the ionization parameter, usually  $O_{32} \equiv (I_{4959} + I_{5007})/I_{3727} = I_{[O\ III]}/I_{[O\ II]}$  as a second parameter (e.g., McGaugh 1991; Pilyugin 2001).

In Figure 3, we compare the equivalent width and flux ratios for the K92+ galaxies (crosses) and NFGS galaxies (solid symbols). For completeness sake, on the left we plot  $W_{[O III]}/W_{[O II]}$  against the observed  $F_{[O III]}/F_{[O II]}$  ratio; there is a clear correlation, but the points are scattered mostly below the 1-to-1 correlation (shown by the line), consistent with the lack of reddening correction. Residuals to the 1-to-1 line are shown in the lower panels, plotted against other galaxy parameters. The strongest correlation is seen against color, which is completely expected: the ratio  $(W_{[O III]}/W_{[O II]})/(F_{[O III]}/F_{[O II]})$  is identical to the ratio of the continua,  $F_{C\lambda 3727}/F_{C\lambda 4959,5007}$ , which will be strongly correlated with  $B - V$ . Most of the other systematic trends in the residuals can be explained as correlations of the other parameters with  $B - V$ .

The right column shows a comparison of equivalent width ratios to the dereddened line ratios. This is of considerable interest, since the ratio  $(W_{[O III]}/W_{[O II]})/(I_{[O III]}/I_{[O II]})$  is a direct measure of  $\alpha$  (see Equation 9). Here there is a much tighter correlation, although there are still some systematic trends in the residuals, again most strongly connected to color. We note, however,  $W_{[O III]}/W_{[O II]}$  is actually very close to  $I_{[O III]}/I_{[O II]}$ , which confirms that  $\alpha$  is near unity on the average. We also note that there appears to be a systematic offset between the NFGS and K92+ galaxies, perhaps related to the offset seen in the NFGS [O III] data (Figure 1, middle column). While we might try to define a color-dependent term for  $\alpha$ , it is unclear how much of the systematic trend is due to the offset between samples. Without any color-dependent term, the scatter in  $\alpha$  about unity is only  $\sigma = 0.12$  dex.

Figure 4 shows the same comparison for the KISS and K92+ samples. Here, the tight relationship between  $B - V$  and the residuals to  $(W_{[O III]}/W_{[O II]})/(F_{[O III]}/F_{[O II]})$  is surprisingly lacking. Since we are effectively comparing  $F_{C\lambda 3727}/F_{C\lambda 4959,5007}$ , measured spectroscopically, with the  $B - V$  color determined from images, this suggests considerable scatter in the continuum measurements. Since the KISS data span a redshift range up to  $0 < z < 0.1$ , it is possible that some of the scatter is due to [O III] contamination of the  $V$  broadband flux, but this would tend to reduce the  $B - V$  colors of those objects with high  $W_{[O III]}$  at higher  $z$ . When we correct for this in a reasonable fashion, we do not see a significant reduction in the scatter, so we must assume the scatter due to some other reason. The cause is almost certainly that the KISS spectroscopy is not integrated across the galaxy, so the spectra tend to be dominated by the nuclear regions, whereas the  $B - V$  colors are from the integrated galaxy light.

Looking at the dereddened line ratios in these data, we do not find any trend in  $\alpha$  with color, although such a trend might be obscured by the scatter. Nevertheless, the scatter about unity is only  $\sigma = 0.14$  dex, and again a value of  $\alpha$  near unity is indicated.

In summary, the local data empirically confirm that adopting  $\alpha = 1$  is a reasonable approximation, with errors around 35%, and therefore the ratio  $W_{[O III]}/W_{[O II]}$  is a reasonable substitute for the ionization parameter,  $I_{[O III]}/I_{[O II]}$ .

### 5.3. $EW R_{23}$ versus $R_{23}$

The previous sections suggest that the equivalent width ratios can be simply substituted into the  $R_{23}$  formula, and here we provide a direct test of that. We define the measure

$$EW R_{23} \equiv \frac{W_{[O II]\lambda 3727} + W_{[O III]\lambda 4959} + W_{[O III]\lambda 5007}}{W_{H\beta}}. \quad (10)$$

which should be approximately equivalent to  $R_{23}$ . For completeness, we will compare  $EW R_{23}$  against both the reddening-corrected  $R_{23}$  and the analogous measure formed with non-corrected line fluxes,  $R_{23}^*$ . Figure 5 (upper left panel) shows the comparison between  $R_{23}^*$  and  $EW R_{23}$  for K92+ and NFGS galaxies constructed from the raw fluxes and equivalent widths. A solid line illustrates a 1-to-1 correspondence. The lower rows in the left column of Figure 5 show residuals from the 1-to-1 correspondence as a function of  $W_{H\beta}$ ,  $W_{[O II]}$ ,  $W_{[O III]}/W_{[O II]}$  and galaxy  $B - V$  color. The correlation between  $R_{23}^*$  and  $EW R_{23}$  is strong but has considerable scatter. Formally, the RMS dispersion from the 1-to-1 relation is  $\sigma(\log[R_{23}^*]) = 0.12$  dex for the combined K92+NFGS samples.

The correlation is strongest for objects in the K92+ sample and for objects with large values of  $R_{23}^*$ . Deviations from 1-to-1 are greatest for objects in the NFGS sample which have low  $W_{H\beta}$ , high  $W_{[O III]}/W_{[O II]}$  ratios, and red colors. These systematic residuals may be understood as a consequence of the lack of corrections for extinction. [O II]  $\lambda 3727$  is significantly affected by extinction compared to the  $H\beta$  and [O III] lines. The measured [O II] flux is a lower limit to the true unextinguished intensity whereas the measured [O II] equivalent width should be unaffected by extinction provided that the extinction toward the gas and stars are similar (but see Calzetti, Kinney & Storchi-Bergmann 1994 for evidence that this assumption is sometimes invalid). The strong systematic residuals with  $B - V$  color seen in the lower left panel is a most likely a consequence uncorrected extinction, since redder galaxies are often those with greater extinction.

In the right column of Figure 5 we show a similar comparison of  $EW R_{23}$  with  $R_{23}$ , where  $R_{23}$  has been corrected for reddening using the theoretical Balmer decrement. Here the correlation is much stronger. The strong correlation between galaxy color and residuals seen in left column is now mostly gone, suggesting that the [O II] line fluxes have been successfully corrected for reddening. The RMS dispersion from the 1-to-1 relation is  $\sigma(\log[R_{23}]) = 0.07$  dex for the combined K92+NFGS samples. The ratio of equivalent widths is a good substitute for the reddening-corrected  $R_{23}$  ratio. Use of equivalent widths will be superior to line ratios if the reddening corrections are not known, as in the case of galaxies for which the  $H\alpha/H\beta$  ratio is not available (typically true for redshifts  $z > 0.3$ ). The residuals in the lower panels of column 2 are mostly symmetric about zero, with the largest scatter again occurring for objects with very low values of  $W_{H\beta}$ . Some of the systematic residuals are probably also caused by varying continuum shapes, especially among the NFGS, which affect the equivalent widths of the [O II] lines in a systematic manner which is related to galaxy color and the average age of the stellar population. In any case, the RMS of 0.07 dex in  $R_{23}$  will often be on the same order as, or even less than the statistical measurement uncertainties on the

strong line equivalent widths in high-redshift spectroscopic surveys, even when the signal-to-noise of the emission line equivalent widths is as low as 8:1.

Figure 6 shows a comparison of  $EW R_{23}$  with  $R_{23}^*$  and  $R_{23}$  for the K92+ and KISS galaxy samples. The left column shows the comparison of  $EW R_{23}$  with  $R_{23}^*$  and the associated residuals from the 1-to-1 correspondence. There is a good correlation between  $EW R_{23}$  with  $R_{23}^*$  in the upper left panel. The RMS dispersion from the 1-to-1 relation is  $\sigma(\log[R_{23}^*]) = 0.11$  dex for the combined K92+KISS samples. The left column shows systematic residuals with galaxy color and line strength indicating that reddening is significant for some galaxies. The right column again shows the comparison of  $EW R_{23}$  with  $R_{23}$  and the associated residuals as a function of equivalent width and galaxy color. The residuals for the KISS galaxies are now slightly smaller and much less systematic after application of a reddening correction. The RMS dispersion from the 1-to-1 relation is  $\sigma(\log[R_{23}]) = 0.09$  dex for the combined K92+KISS samples. The residuals are larger than for the K92+ and NFGS objects, and the KISS galaxies do not show the systematics with galaxy color or line strengths and ratios which the NFGS galaxies exhibit. The lack of systematics with color is attributable to slit-vs-integrated light issues, but this does not explain the larger scatter or lack of systematics with pure line measures. This latter is possibly a result of the relative homogeneity of the KISS sample, as KISS galaxies have stronger emission lines and do not include the diversity of more quiescent galaxies with older stellar populations found in the NFGS.

### 5.3.1. Effects of Stellar Balmer Absorption

Ideally, the quantity  $R_{23}$  from which a metallicity is derived should be computed using an  $H\beta$  line strength which has been corrected for both interstellar reddening *and* absorption by atmospheres of the underlying stellar population. In practice, the amount of underlying absorption is difficult to measure even under ideal circumstances with high signal-to-noise data. Spectra of distant galaxies frequently lack the signal-to-noise necessary to measure multiple Balmer lines and correct simultaneously for extinction and Balmer absorption in a self-consistent fashion. For galaxies with strong emission lines due to active star formation (i.e.,  $W_{H\beta} > 25 \text{ \AA}$ ), a correction of a few  $\text{\AA}$  to the  $H\beta$  line will have a small impact on the derived  $R_{23}$  or  $EW R_{23}$ . However, in galaxies dominated by older stellar populations with weak emission lines,  $R_{23}$  or  $EW R_{23}$  will depend sensitively on the correction for Balmer absorption.

Until this point in the analysis, we have not made any corrections for stellar Balmer absorption. The effect of underlying Balmer absorption (specifically the amount of absorption in the  $H\beta$  line,  $W_{H\beta}(abs)$ ) will depress the measured  $F_{H\beta}$  and  $W_{H\beta}$ . This leads to systematically large  $R_{23}$  or  $EW R_{23}$ , and systematically low oxygen abundances for objects on the upper (metal-rich) branch of the empirical calibrations.

The impact of stellar absorption can be assessed using Figure 7. Using the K92+ galaxy spectra, we measured several Balmer lines and performed a self-consistent reddening and stellar

absorption solution for each galaxy (see Kobulnicky & Skillman, 1996, for additional details). The results indicated a range in underlying  $H\beta$  absorption of  $\sim 1\text{--}3 \text{ \AA}$  with an average value near  $2 \text{ \AA}$ . From these data we calculate a quantity  $R_{23}^+$  which includes the corrections for reddening and stellar absorption calculated for each galaxy. The upper left panel of Figure 7 compares the “raw”  $EW R_{23}$  ratio with the quantity  $R_{23}^+$ ; the correlation is modest, with a dispersion of  $\sigma(R_{23}^+) = 0.14$  dex and a systematic offset of 0.06 dex. The lower panels illustrate the nature of the residuals as a function of galaxy color and line strengths. As might be expected, galaxies with the lowest  $W_{H\beta}$  are the most deviant, while galaxies with  $W_{H\beta} > 20$  show a much smaller dispersion. A more logical approach is also to add a correction to  $W_{H\beta}$  for the underlying stellar absorption, forming a new quantity  $EW R_{23}^+$ . A  $2 \text{ \AA}$  correction to  $W_{H\beta}$  was chosen because it was the mean correction needed to produce  $R_{23}^+$ , and is consistent with mean corrections found for other galaxies (e.g., McCall *et al.* 1985; Olofsson 1995). The right top panel shows  $EW R_{23}^+$  plotted against  $R_{23}^+$ . The residuals are now much smaller with  $\sigma(R_{23}^+) = 0.08$  dex and a systematic offset of less than 0.01 dex. In the absence of direct measurements of the Balmer absorption due to stellar populations, application of a  $2 \text{ \AA}$  blanket correction to  $W_{H\beta}$  appears to be prudent for the types of starforming galaxies in the K92+, DGSS and KISS samples. Samples including galaxies with older stellar populations may require larger corrections.

## 6. Discussion and Conclusions

The ratios of the equivalent widths of strong oxygen and hydrogen emission lines from the ionized component of distant galaxies can be used as a measure of the global ISM metallicity via the substitution of  $EW R_{23}$  for  $R_{23}$ . We recommend the use of  $EW R_{23}^+$  where the  $W_{H\beta}$  has been corrected for stellar Balmer absorption assuming a mean correction of  $2 \text{ \AA}$ . The typical dispersion from the 1-to-1 relation between either  $EW R_{23}$  or  $EW R_{23}^+$  and the canonical reddening and absorption-corrected  $R_{23}$  ratio is  $\sigma(R_{23}) = 0.08$  dex. Residuals are somewhat smaller ( $\sigma = 0.05$  dex) for galaxies with the largest emission-line equivalent widths (i.e., those having the largest rates of star formation per unit luminosity). The translation of these errors into errors in oxygen abundance will depend on the value of  $R_{23}$ , but for the upper-metallicity branch away from the “turnaround” point, the slope of  $\log(\text{O}/\text{H})$  vs  $\log(R_{23})$  is  $\sim 1.4$  (Pilyugin 2001), so the addition error in  $\log(\text{O}/\text{H})$  would be  $\sim 0.11$  dex. Thus, the additional uncertainty introduced by translating a set of measured equivalent widths into the traditional  $R_{23}$  flux ratio diagnostic is comparable to or less than the typical observational line measurement uncertainties and systematic errors in the  $R_{23}$  to O/H calibration which run 0.15 dex in O/H (e.g., Kobulnicky, Kennicutt & Pizagno 1999 for a more detailed discussion of the error budget). We anticipate that the method tested here will be useful for performing rough chemical abundance estimates in large high-redshift galaxy samples. The approach described here will be most useful in a statistical sense when large numbers of objects are available for study. Possible applications include understanding the overall chemical evolution of star forming galaxies over large intervals of cosmic time (Kobulnicky *et al.* 2003) or assessing the impact of cluster environment and the intracluster medium on the chemical properties of the

ISM within galaxies (e.g., Skillman *et al.* 1996).

John Salzer helped make this paper possible by providing the KISS data in tabulated form and by commenting on the manuscript. Detailed comments by an anonymous referee greatly improved the manuscript. We thank Sheila Kannappan for a helpful discussion about the NFGS. H. A. K. was supported by NASA through grant #HF-01090.01-97A awarded by the Space Telescope Science Institute which is operated by the Association of Universities for Research in Astronomy, Inc. for NASA under contract NAS 5-26555. This work was also made possible by funding from the National Science Foundation through grant AST-9529098, and NASA through NRA-00-01-LTSA-052.

A. C. P. would like to dedicate this paper to Gary Grasdalen, an early mentor, with thanks.

## REFERENCES

- Aller, L. H. 1990, *PASP*, 102, 1097
- Calzetti, D., Kinney, A. L., & Storchi-Bergmann, T. 1994, *ApJ*, 429, 582
- Dopita, M. A., & Evans, I. N. 1986, *ApJ*, 307, 431
- Edmunds, M. G. & Pagel, B. E. J. 1984, *MNRAS*, 211, 507
- Howarth, I. D. 1983, *MNRAS*, 203, 301
- Huchra, J. P., Davis, M., Latham, D., & Tonry, J. 1983, *ApJS*, 52, 89
- Hummer, D. G., & Storey, P. J. 1987, *MNRAS*, 224, 801
- Jansen, R. A., Franx, M., Fabricant, D., & Caldwell, N. 2000a, *ApJS*, 126, 271 (NFGS)
- Jansen, R. A., Fabricant, D., Franx, M., & Caldwell, N. 2000b, *ApJS*, 126, 331
- Kennicutt, R. C. Jr. 1992a, *ApJS*, 79, 255
- Kennicutt, R. C. Jr. 1992b, *ApJ*, 388, 310
- Kobulnicky, H. A., Kennicutt, R. C., & Pizagno, J. 1998, *ApJ*, 514, 544 (KKP)
- Kobulnicky, H. A. & Gebhardt, K. 2000, *AJ*, 119, 1608
- Kobulnicky, H. A., Willmer, C. N. A., Weiner, B. J., Koo, D. C., Phillips, A. C., Faber, S. M., Sarajedini, V. L., Simard, L., & Vogt, N. P. 2003, *ApJ*, 000 (Ke03)
- Kobulnicky, H. A., & Skillman, E. D. 1996, *ApJ*, 471, 211
- McCall, M. L., Rybski, P. M., & Shields, G. A. 1985, *ApJS*, 57, 1 (MRS)
- McGaugh, S. 1991, *ApJ*, 380, 140
- McGaugh, S. 1998, private communication
- Melbourne, J., & Salzer, J. J. 2002, *AJ*, 123, 2302
- Morgan, W. W., & Mayall, N. U. 1957, *PASP*, 69, 291

- Olofsson, K. 1995, A&AS, 111, 570
- Osterbrock, D. E. 1989, *Astrophysics of Gaseous Nebulae and Active Galactic Nuclei*, University Science Books:Mill Valley CA
- Pagel, B. E. J. 1998, *Nucleosynthesis and Chemical Evolution of Galaxies*, Cambridge University Press
- Pagel, B. E. J. Edmunds, M. G., Blackwell, D. E., Chun, M. S., & Smith, G. 1979, MNRAS, 189, 95
- Pilyugin, L. S., 2001, A&A, 369, 594
- Pritchett, C. R. 1977, ApJS, 35, 397
- Salzer, J. J. 2003, private communication
- Salzer, J. J. *et al.* 2003, in press
- Salzer, J. J., Gronwall, C., Lipovetsky, V. A.; Kniazev, A., Moody, J. W., Boroson, T. A., Thuan, T. X., Izotov, Y. I., Herrero, J. L., Frattare, L. M. 2000, AJ, 120, 80 (KISS)
- Seaton, M. J. 1979, MNRAS, 187, 73p
- Skillman, E. D., Kennicutt, R. C., Shields, G. A., & Zaritsky D. 1996, ApJ, 462, 147

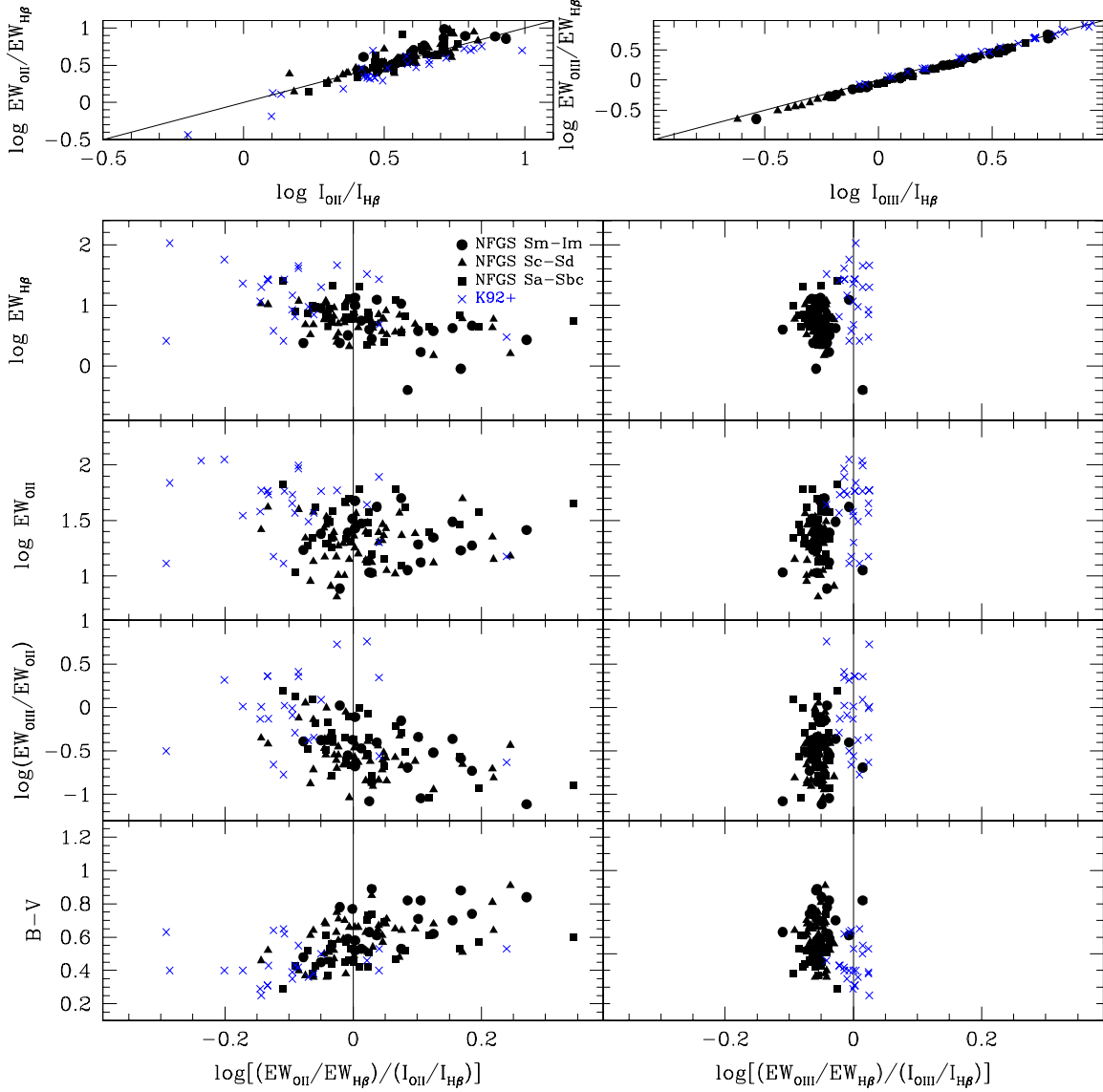


Fig. 1.— Comparison of dereddened emission line fluxes and flux ratios to emission line equivalent widths and EW ratios for galaxies from Kennicutt (1992a,b) and Jansen *et al.* (2000a,b; NFGS). Upper panels show the  $[O\ II]/H\beta$  flux ratios and EW ratios with a line illustrating the 1-to-1 correspondence. Lower panels show residuals from the 1-to-1 relation as a function of equivalent width and galaxy color. There is generally a strong correlation between flux ratios and EW ratios. Panels showing systematic residuals are discussed in the text. Note that the ratio  $(W_{[O\ II]}/W_{H\beta})/(I_{[O\ II]}/IH\beta)$  is a measure of  $1/\alpha$ .

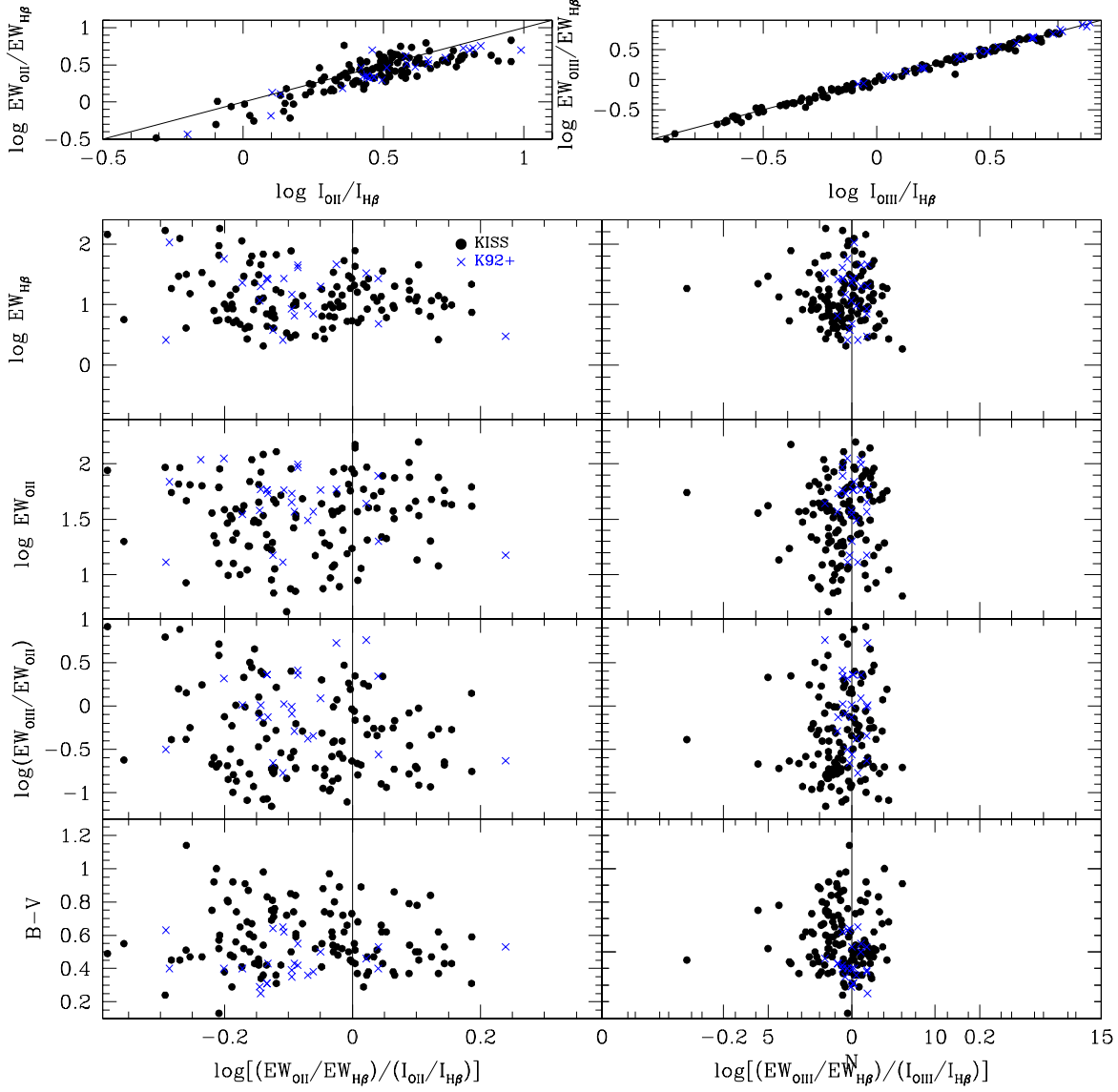


Fig. 2.— Comparison of dereddened emission line fluxes and flux ratios to emission line equivalent widths and EW ratios for galaxies from the K92+ galaxies and the KISS (Salzer *et al.* 2001) emission line galaxy survey. Upper panels show the [O II]/H $\beta$  flux ratios and EW ratios with the line illustrating the 1-to-1 correspondence. Lower panels show residuals from the 1-to-1 relation as a function of equivalent width and galaxy color. There is generally a strong correlation between flux ratios and EW ratios. Panels showing systematic residuals are discussed in the text.

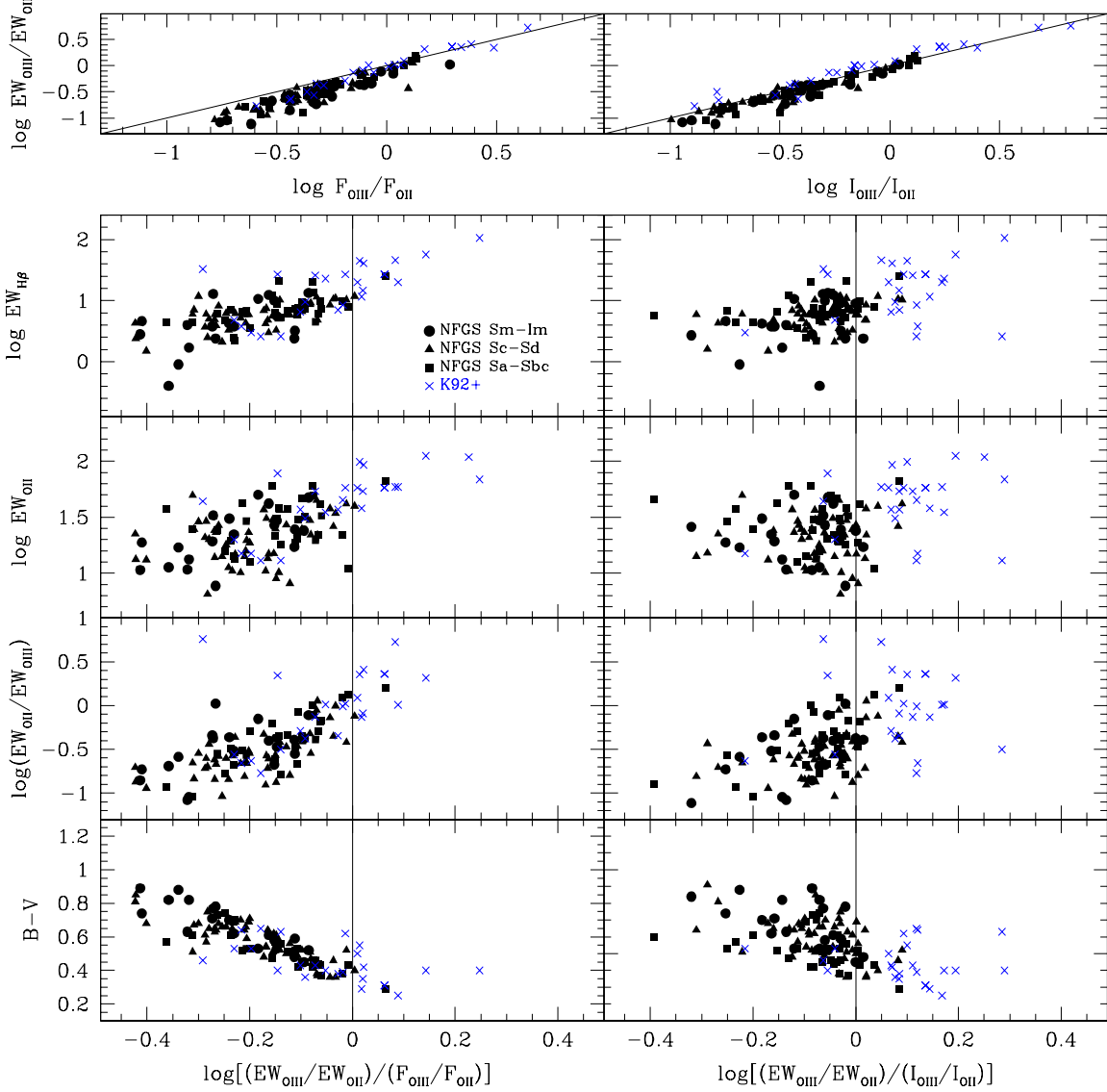


Fig. 3.— Comparison of the ionization parameter quantity  $W_{[O III]}/W_{[O II]}$  with  $F_{[O III]}/F_{[O II]}$  and the dereddened ratio  $I_{[O III]}/I_{[O II]}$  for the K92+ and NFGS galaxies. Lower panels show the residuals from the 1-to-1 correspondence as a function of line strength and galaxy color. The tight correlation between  $(W_{[O III]}/W_{[O II]})/(F_{[O III]}/F_{[O II]})$  and  $(B - V)$  is expected, as the latter simply represents the ratio of spectroscopically measured continuum flux under the lines. The ratio  $(W_{[O III]}/W_{[O II]})/(I_{[O III]}/I_{[O II]})$  gives the unknown value  $\alpha$ .

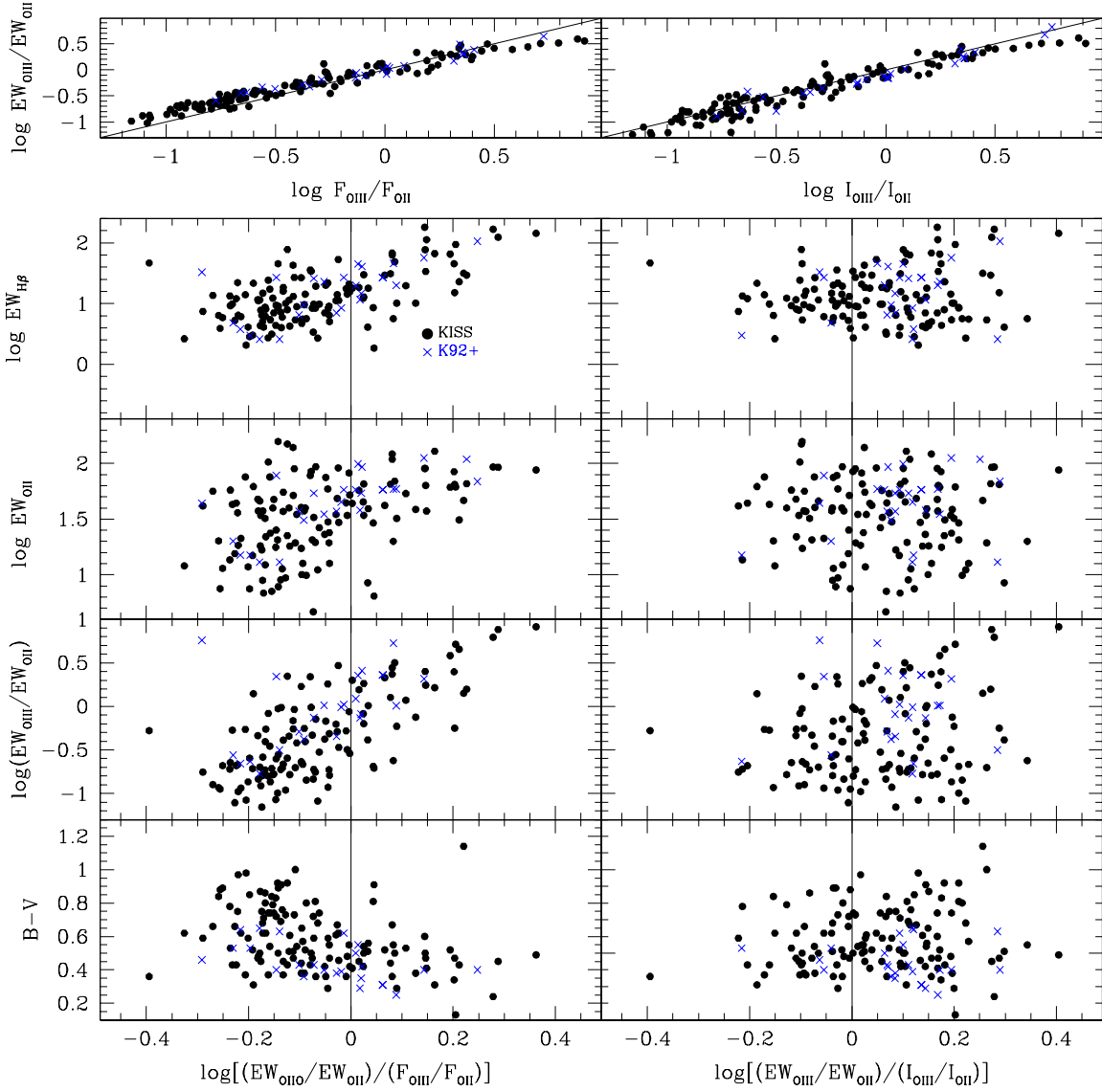


Fig. 4.— Same as Figure 3 except with KISS in place of NFGS galaxies. The lack of a tight correlation between  $(B-V)$  and  $(W_{[\text{O III}]} / W_{[\text{O II}]}) / (F_{[\text{O III}]} / F_{[\text{O II}]})$  is most likely due to observing different regions of each galaxy for spectroscopy and photometry (see text).

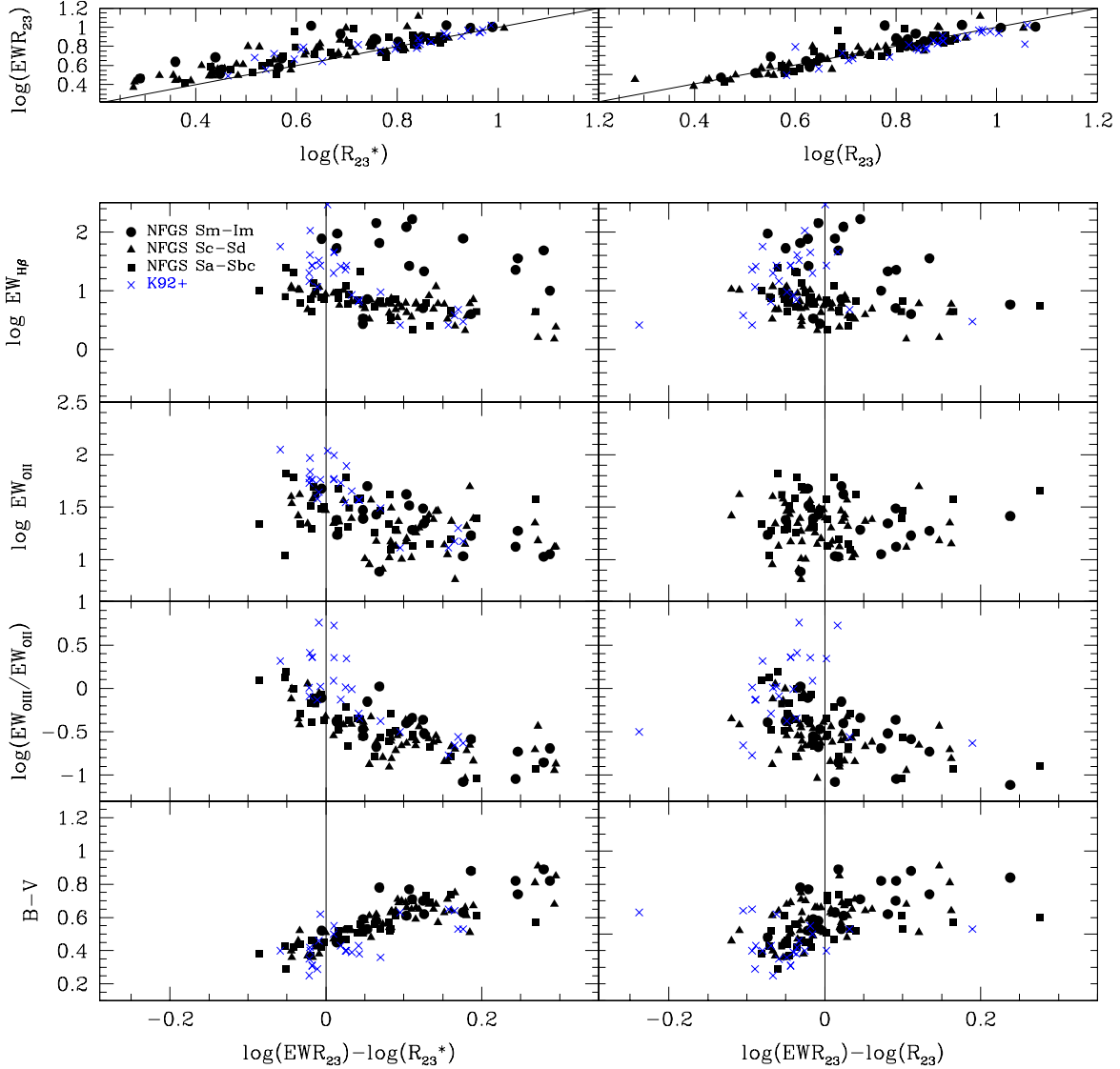


Fig. 5.— Comparison of the quantity  $R_{23}$  and  $R_{23}^*$  with  $EWR_{23}$ .  $R_{23}^*$  is  $R_{23}$  without correction for reddening. The strong correlation between  $R_{23}^*$  and  $EWR_{23}$  (upper left panel) is even stronger for  $R_{23}$  and  $EWR_{23}$ , suggesting that oxygen abundances can be estimated from equivalent width ratios as well as from dereddened line fluxes. The improvement of the correlation with  $R_{23}$  shows that  $EWR_{23}$  is successful in correcting at least part of the reddening. The RMS dispersion from the 1-to-1 relation is  $\sigma(\log[R_{23}]) = 0.07$  dex. Lower panels explore the residuals in the correlation as a function of line strength, line ratio, and galaxy color. *left column*: no correction for extinction or underlying Balmer absorption in either quantity; *right column*: line fluxes have been corrected for reddening. There remains a small systematic trend with color, but, excluding only a few outliers, the  $EWR_{23}$  and  $R_{23}$  values agree to about  $\pm 0.1$  dex for this sample.

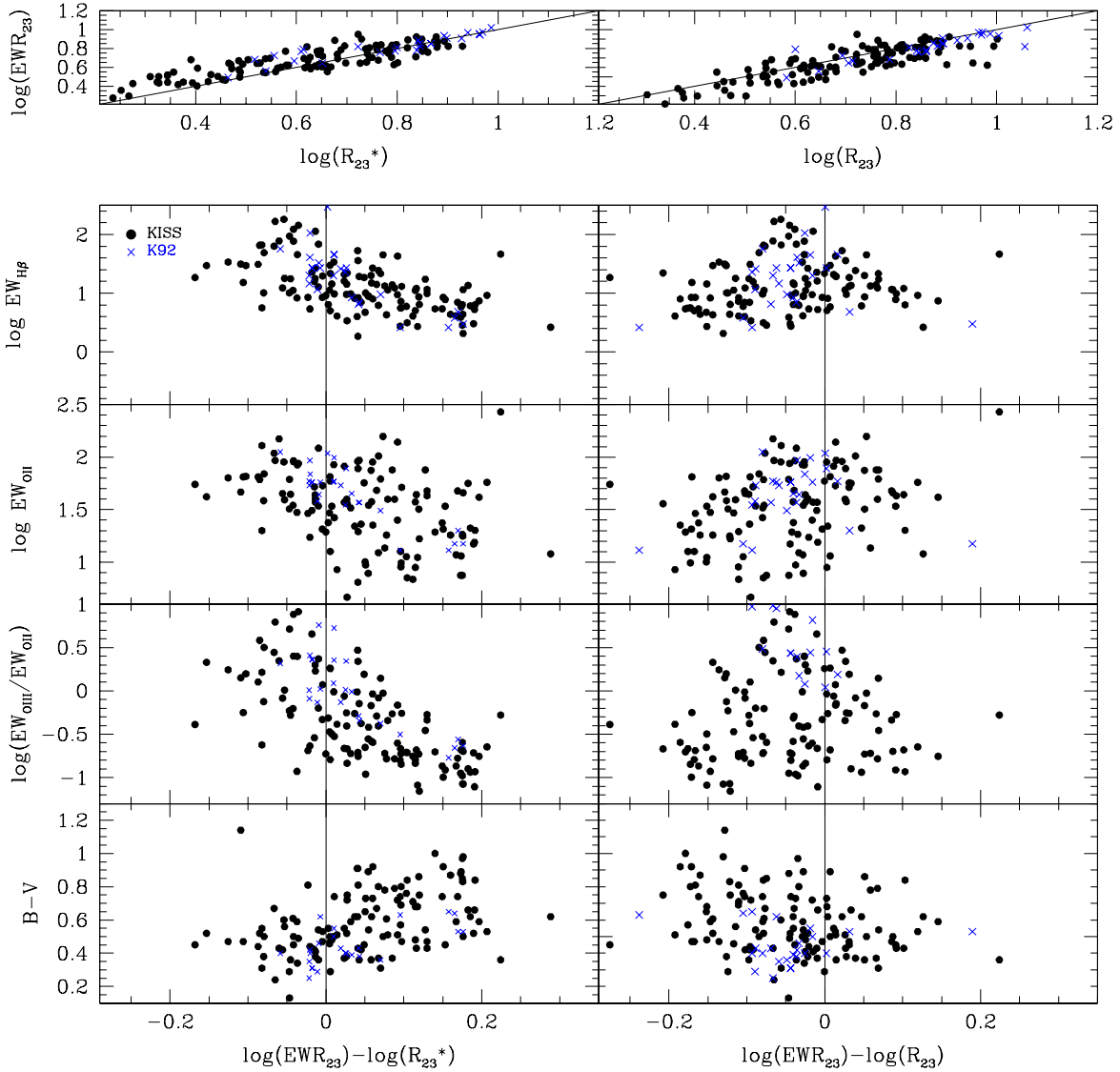


Fig. 6.— Comparison of the quantity  $R_{23}$  and  $R_{23}^*$  with  $EWR_{23}$  for the K92+ and KISS galaxy samples. Upper panels show the excellent correlation between  $R_{23}$  and  $R_{23}^*$  with  $EWR_{23}$ . Lower panels show the residuals from the 1-to-1 correspondence as a function of line strength and galaxy color. Residuals are larger, but less systematic, for the KISS galaxies than for the NFGS and K92+ galaxies.

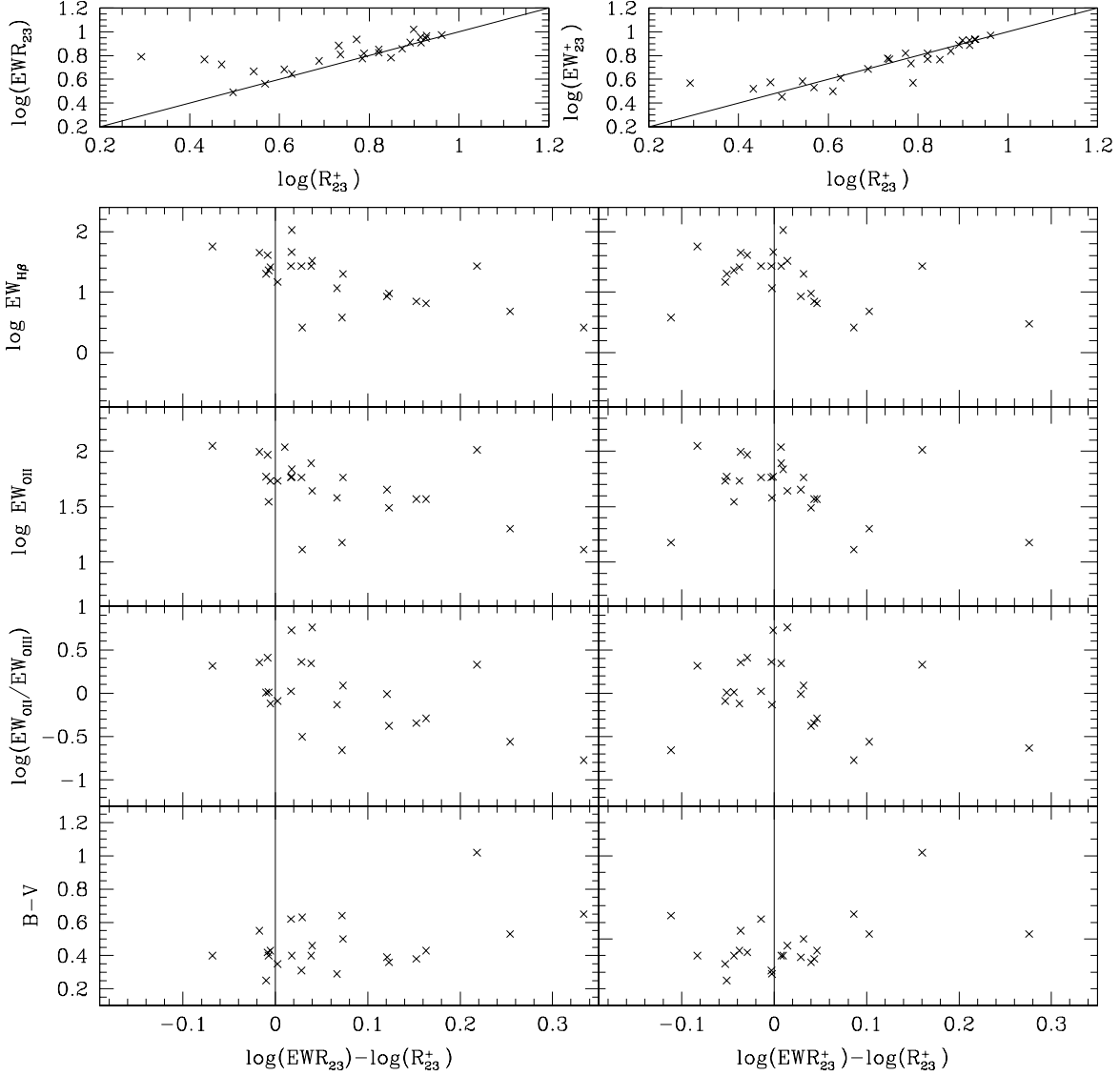


Fig. 7.— Effects of correcting for underlying  $H\beta$  absorption in K92+ galaxies. The quantities  $R_{23}^+$  and  $EWR_{23}^+$  are analogous to  $R_{23}$  and  $EWR_{23}$  but with the  $H\beta$  measurements corrected for stellar absorption by  $2 \text{ \AA}$ , an average value found in a self-consistent fit to both the reddening and stellar absorption using the available Balmer lines (see text). Upper panels show the correlation between  $R_{23+}$  and with  $EWR_{23}$  and  $EWR_{23+}$ . Lower panels show the residuals from the 1-to-1 correspondence as a function of line strength and galaxy color. Galaxies with  $W_{H\beta} \leq 15 \text{ \AA}$  are most seriously affected by the lack of correction for stellar absorption.